

We are IntechOpen, the world's leading publisher of Open Access books Built by scientists, for scientists

6,900

Open access books available

186,000

International authors and editors

200M

Downloads

Our authors are among the

154

Countries delivered to

TOP 1%

most cited scientists

12.2%

Contributors from top 500 universities



WEB OF SCIENCE™

Selection of our books indexed in the Book Citation Index
in Web of Science™ Core Collection (BKCI)

Interested in publishing with us?
Contact book.department@intechopen.com

Numbers displayed above are based on latest data collected.
For more information visit www.intechopen.com



Regional Climate Model Applications for West Africa and the Tropical Eastern Atlantic

Leonard M. Druyan and Matthew Fulakeza
*Center for Climate Systems Research, Columbia University,
NASA/Goddard Institute for Space Studies, New York,
USA*

1. Introduction

The chapter reviews applications of a regional climate model for studies of climate variability over West Africa and the adjacent eastern tropical Atlantic Ocean. Fig. 1a shows the region and identifies some of the geographic features mentioned in the chapter. The savannah region south of the Sahara Desert, known as the Sahel (situated between 10-15°N), is of particular interest to climate scientists because of its vulnerability to recurring drought. The West African monsoon (WAM) is characterized by the advance of precipitation northward to the Sahel region during late June or early July (onset) and its southward retreat during September. Below normal Sahel rainfall during some summers is associated with an abbreviated northward advance of this rain belt (Hastenrath and Polzin, 2010). A shortfall in seasonal rainfall has an especially severe negative impact on the pastoral and agricultural economies of the region, causing famine and widespread social upheaval in worst case scenarios. The socio-economic repercussions of drought or even floods lend importance to the ultimate goals of climate model research relevant to this area: improving seasonal forecasts, predicting monsoon onset dates, determining the role of sea-surface temperature anomalies and land surface characteristics on the variability of the developing monsoon and creating reliable projections of the future Sahel climate under a range of greenhouse warming scenarios. Early warning of imminent drought, for example, can allow mitigation strategies to blunt some of the negative impacts. In addition, research is also devoted to better understanding African easterly wave disturbances (AEWs). AEWs enter the tropical Atlantic from West Africa during the summer and can develop into tropical cyclones, and occasionally into hurricanes.

Regional climate models (RCMs) are integrated over limited area domains. Accordingly, RCMs can afford higher horizontal resolution than global domain models for the same dedication of computer resources. Computation over the limited area domains alternatively facilitates multiple and longer simulations. The usually higher horizontal resolution of RCMs (compared to global models) offers the potential for better definition of spatial gradients of topography, land surface characteristics and the atmospheric variables involved in the models' integration and output. More accurate gradients, in turn, improve the simulations and provide better detail in the modeled results of interest to users of climate data.

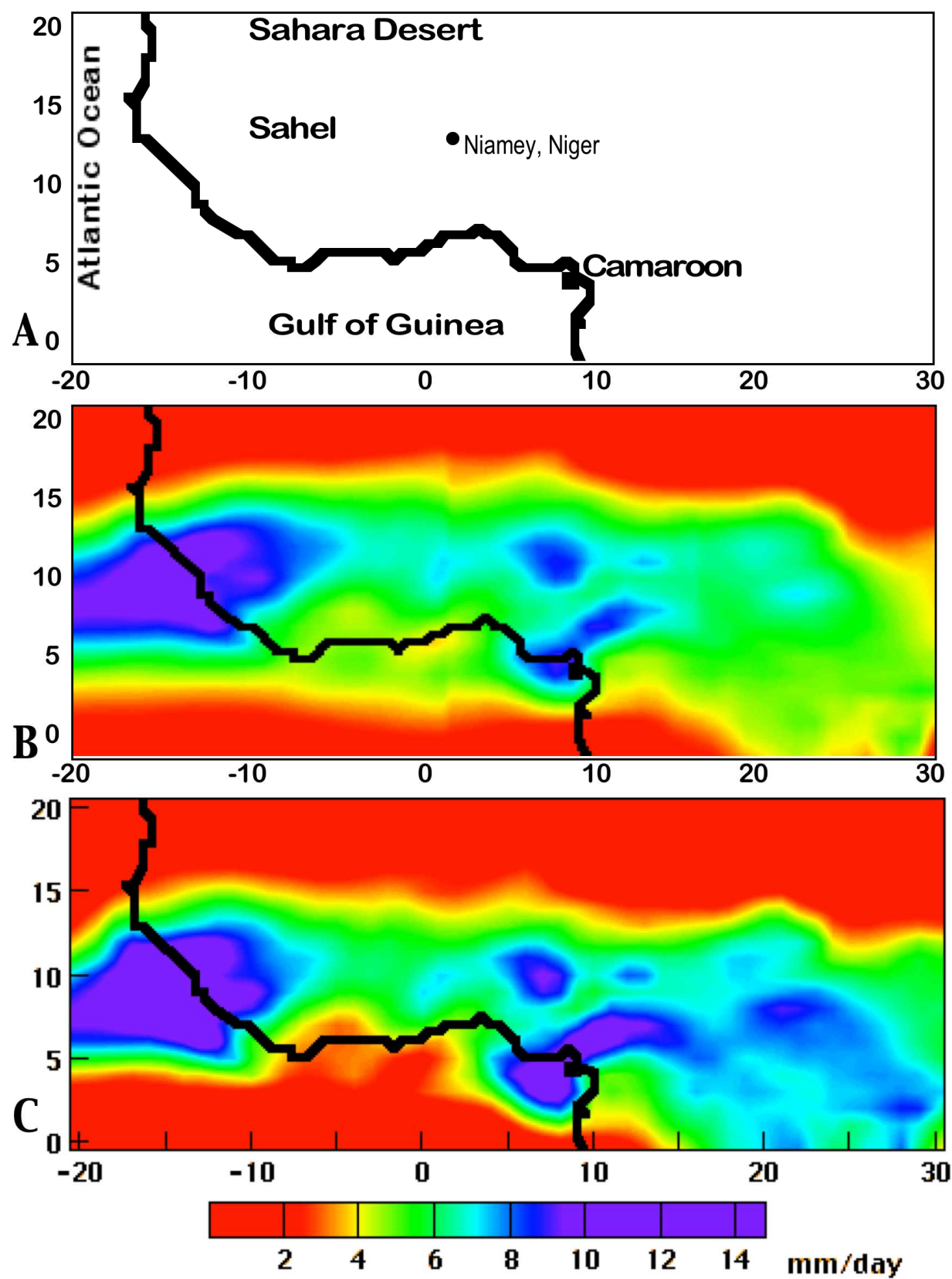


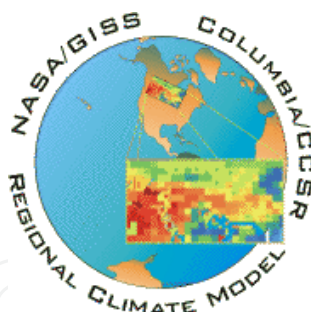
Fig. 1. a. Geography of West Africa. b. Mean RM3 16L precipitation rates (mm day⁻¹) for June-September 1998-2003, c. corresponding TRMM means (courtesy of NASA's Goddard Earth Sciences [GES] Data and Information Services Center).

For example, better resolution of the exceptionally strong and dynamically important summertime meridional temperature and moisture gradients south of the Sahara should contribute to more skillful simulations than are possible using coarser gridded global models. In addition, projected rainfall distributions mapped on a 0.5° grid are much more useful for agricultural applications than corresponding data on a 2.5° grid. The chapter gives a detailed description of one such RCM applied to WAM studies.

Although some model-based climate studies focus only on monthly or seasonally mean fields, confidence in results improves if the models realistically capture the characteristics of relevant daily weather phenomena. For example, precipitation triggered and modulated by transient AEWs plays a crucial role in West African summer monsoon hydrology. Accordingly, modeling the behavior of AEWs is a fruitful application of RCMs, made more meaningful by validation against corresponding observational evidence. The chapter describes RCM simulations of AEWs and their associated precipitation patterns.

2. The regional climate model of the Center for Climate Systems Research (CCSR, Columbia University) and the NASA/Goddard Institute for Space Studies in New York City (GISS)

Druyan et al. (2006) and Druyan et al. (2008) describe the regional climate model (3rd generation version), the *RM3*, which runs exclusively at CCSR/GISS. The authors have published some 13 papers since 2000 describing various characteristics of RM3 climate simulations. The earlier version integrated the equations of motion at 16 vertical sigma levels, while the current version of the RM3 has been expanded to 28 vertical sigma levels. The RM3 was improved over the years by incorporating land surface hydrology and moist convection modules originally developed for the global climate model of NASA/GISS.



Model computations are made on a horizontal grid with either 0.5° latitude/longitude spacing, or, for the currently underway CORDEX (Coordinated Regional Climate Downscaling Experiment) simulations, 0.44° grid spacing. Given typical AEW wavelengths of 2800 km (25° longitude), these grid resolutions resolve AEWs quite well and can also represent mesoscale convective complexes imbedded within AEWs. Integration of the RM3 simulates the 4-D evolution of atmospheric temperature, humidity and circulation as well as the location, rate and timing of precipitation.

The RM3 incorporates a land surface (LS) process model, originally developed by Rosenzweig and Abramopoulos (1997) (See also Hansen et al. 2002), that computes ground temperatures, soil moisture variability and evapotranspiration. The LS model consists of two integrated parts, the soil and the canopy, and it conserves water and heat while

simulating their vertical fluxes. The RM3 modeled soil is divided into six layers to a depth of 3.5 m, and the model distinguishes between five textures of soil. The canopy, modeled as a separate layer located above the soil, is responsible for the interception of precipitation, evaporation of accumulated water and removal of soil water through transpiration. Ocean temperatures are specified boundary data that are updated daily, usually from the same data set that provides the lateral boundary conditions.

The DelGenio and Yao (1993) moist convection parameterization and the Del Genio et al. (1996) scheme for the effects of cloud liquid water are important RM3 modules. The convection scheme incorporates entraining and non-entraining plumes, downdrafts, and subsidence. Vertical cumulus mass fluxes are proportional to the moist static stability and are constrained to relax the atmosphere to a neutrally stable state at the cloud base. The convective plume and subsiding environment transport grid-scale horizontal momentum. Convective cloud cover is assigned as proportional to the mean pressure thickness of all model layers up to the cloud top. The cloud liquid water scheme (DelGenio et al., 1996) allows for life cycle effects in stratiform clouds and permits cloud optical properties to be determined interactively. Cloud optical thickness is calculated from the predicted liquid/ice water path and a variable droplet effective radius estimated by assuming constant droplet number concentration. Microphysical and radiative properties are assumed to be different for liquid and ice clouds, and for liquid clouds over land and ocean. Mixed phase processes can change the phase if ice falls into a lower layer containing supercooled liquid water. The scheme parameterizes Bergeron-Findeisen diffusional growth of the ice phase at the expense of the liquid phase via the "seeder-feeder" process by allowing a layer with supercooled water to glaciare if sufficient ice falls into it from above.

Three RM3 domains for simulations are used. For the Druyan and Fulakeza (2011) study of systems in the tropical eastern Atlantic, the domain for the 0.5° grid is 20°S-35°N, 50°W-20°E, representing a westward shift of 15° of longitude relative to the domain used by Druyan et al. (2008), which focuses more on West Africa. CORDEX simulations are made over a 0.44° grid domain expanded to include all of Africa and adjacent coastal oceans: 50°S-50°N, 35°W-64°E.

Atmospheric boundary conditions and SST to drive the RM3, for most of the published studies, are taken from the US National Center for Environmental Prediction and Department of Energy reanalysis (NCPR, 1 and 2), archived at 2.5° latitude/longitude grid spacing (Kanamitsu et al. 2002). Driving the RCM with NCPR is not appropriate for any of several important applications: not for daily weather predictions, nor seasonal climate outlooks, nor for investigating the implications of decadal climate change on a regional scale. However, the analysis of downscaling NCPR does enable an assessment of whether the RCM can successfully provide more realistic spatial detail of climate variables than the driving data set. Over West Africa in August, this could mean generating and propagating a squall line that is not resolved at 2.5° grid spacing. Optimization of the RCM downscaling of NCPR then provides a better RCM tool, which can subsequently be driven by boundary conditions from global models' weather or climate forecasts or decadal climate projections, for the stated applications. Moreover, the RM3/NCPR system can also be used to test the sensitivity of the local climate to prescribed changes in SST and/or land surface conditions or to modeling changes.

3. Results of selected RM3 experiments

Druyan et al. (2006) describe the results of RM3 16L (16 level version) simulations spanning six summers (June-September), 1998-2003. Initial conditions for each seasonal run are NCPR atmospheric, soil moisture and SST data for May 15. RM3 simulations on the 0.5° grid are then driven by synchronous NCPR lateral boundary data and sea-surface temperatures, four times daily, interpolated to the RM3 grid.

Six-year mean June-September RM3 precipitation is validated against gridded observational data from the Climate Research Unit (CRU) of East Anglia University (New et al. 2002) as well as against data from the Tropical Rainfall Measuring Mission satellite- TRMM (3B43 V6) (Kummerow et al., 2000). All data sets were gridded at 0.5° latitude/longitude. Figs. 1b and 1c show that the RM3 reproduces the TRMM observed orographic precipitation maxima along the southwest (Guinea) coast and over coastal Cameroon, albeit with some underestimates. It also features the West African rain belt along 10°N , although too much precipitation is simulated along the Gulf of Guinea coast, which climatologically experiences a dry period in August.

3.1 RM3 daily precipitation time series compared to rain gauges and TRMM

Daily precipitation variability across the Sahel in summer is to a large measure regulated by the transit of AEWs. Time series of RM3 and TRMM (3B42 V6) simulated daily precipitation accumulations are compared to a time series of co-located rain gauge measurements near Niamey, Niger (from Thorncroft et al. 2003), in Fig. 2. Niamey is identified on the map in Fig. 1a.

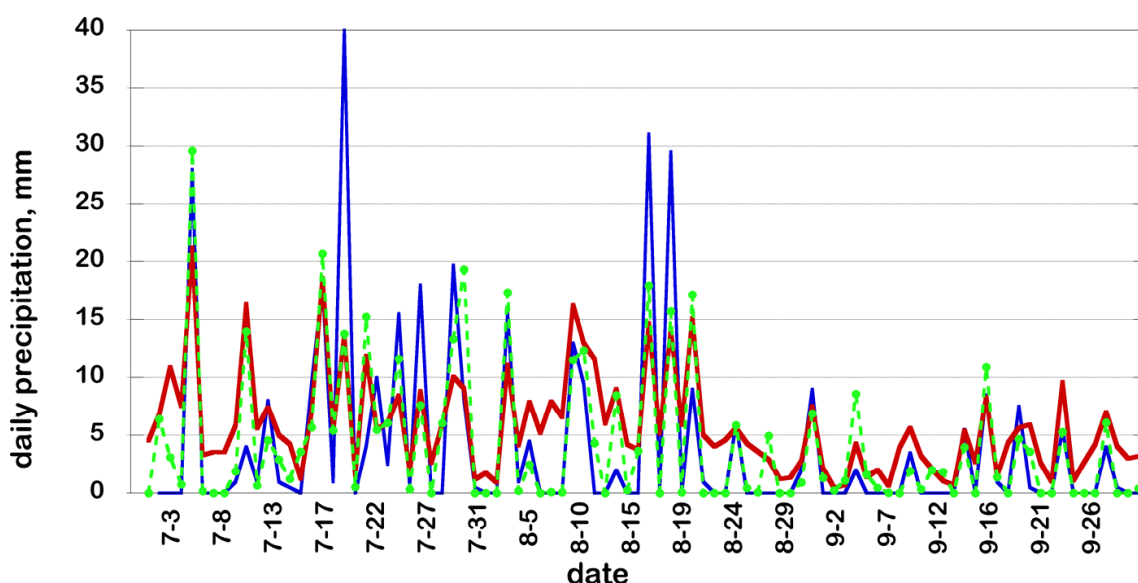


Fig. 2. Time series of the mean of 34 rain gauge observations (blue) within the area bounded by $13-13.9^\circ\text{N}$, $1.7-3.1^\circ\text{E}$ (Thorncroft et al. 2003) versus RM3 daily values (red) for 15 co-located grid elements and TRMM daily estimates (green) for four co-located 1° squares, July-September 2000.

Note that the RM3 and TRMM represent area averages, compared to the average of 34 single point observations of the rain gauges. One model deficiency is that, even on days observed to be rainless, RM3 daily precipitation is non-zero. However, the model simulation does

indicate a peak on every rainy day, and many of the peaks are comparable to observations. There are three days on which much larger accumulations were measured by rain gauges than indicated by the RM3 or by TRMM. The correlation of the 3-month time series of the RM3 simulation versus TRMM is 0.86. The correlation between the rain gauge time series and TRMM is 0.79, and between the RM3 and the rain gauges, 0.73. Thus, both TRMM and the RM3 produce a daily variability that matches rain gauge measurements quite well. Note that the RM3/NCPR system does not share any data source with the TRMM system so that all three sources of precipitation data are completely and mutually independent.

3.2 The spectral signature of AEWs

AEW-related vorticity is particularly strong at 700 mb, just below the level of the African Easterly Jet. Transient AEWs cause perturbations in the 700 mb meridional wind (v_7), related to their cyclonic circulation. Time series of v_7 at a given West African location therefore exhibit a periodicity determined by the frequency of AEW traversal. Spectra of v_7 time series at such locations show peaks for periods ranging between 3-6 days, which are the spectral signature of AEWs. The example shown in Fig. 3, for the location 15°N , 12°W , is from a RM3 16L simulation forced by NCPR data for June-September 2002. This particular example shows spectral peaks at 3.9 and 5.1 days. Spatial mapping of the spectral amplitudes between 3-6 days indicates preferred AEW tracks.

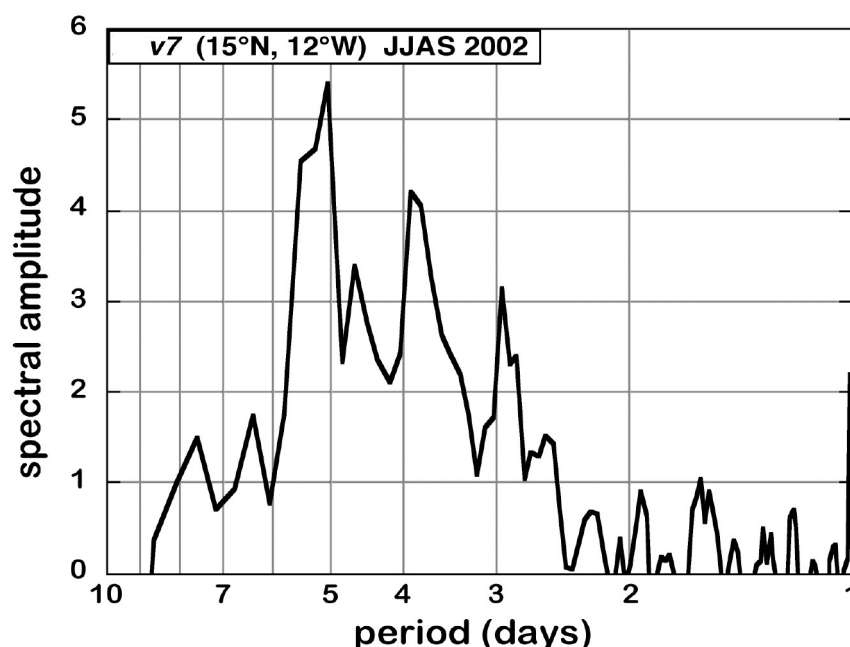


Fig. 3. Spectrum for June-September 2002 time series of RM3 16L simulated v_7 at 15°N , 12°W . The red noise spectrum has been subtracted. Peaks at 3.9 days and 5.1 days reflect the periodicity of v_7 due to the traversal of AEWs.

RM3 700 mb circulation shows evidence of considerable interannual variability in spectral properties that relate to AEWs. Spectral amplitudes for 700 mb meridional wind time series peak most often in the range of 3-6- day periods over swaths traversed by AEWs. RM3 results favor AEW tracks near 17°N and 5°N .

3.3 Validation of RM3 daily circulation variability

AEWs are also manifest by westward propagating bands of alternating southerlies and northerlies in NCPR, European Center for Medium- range Weather Forecasting 40- year reanalysis (ERA-40) and RM3 700 mb circulations. Fig. 4 shows time series of once daily v_7 , averaged over 5-15°N along 7.5°W, for each of six Augusts from the three data sets.

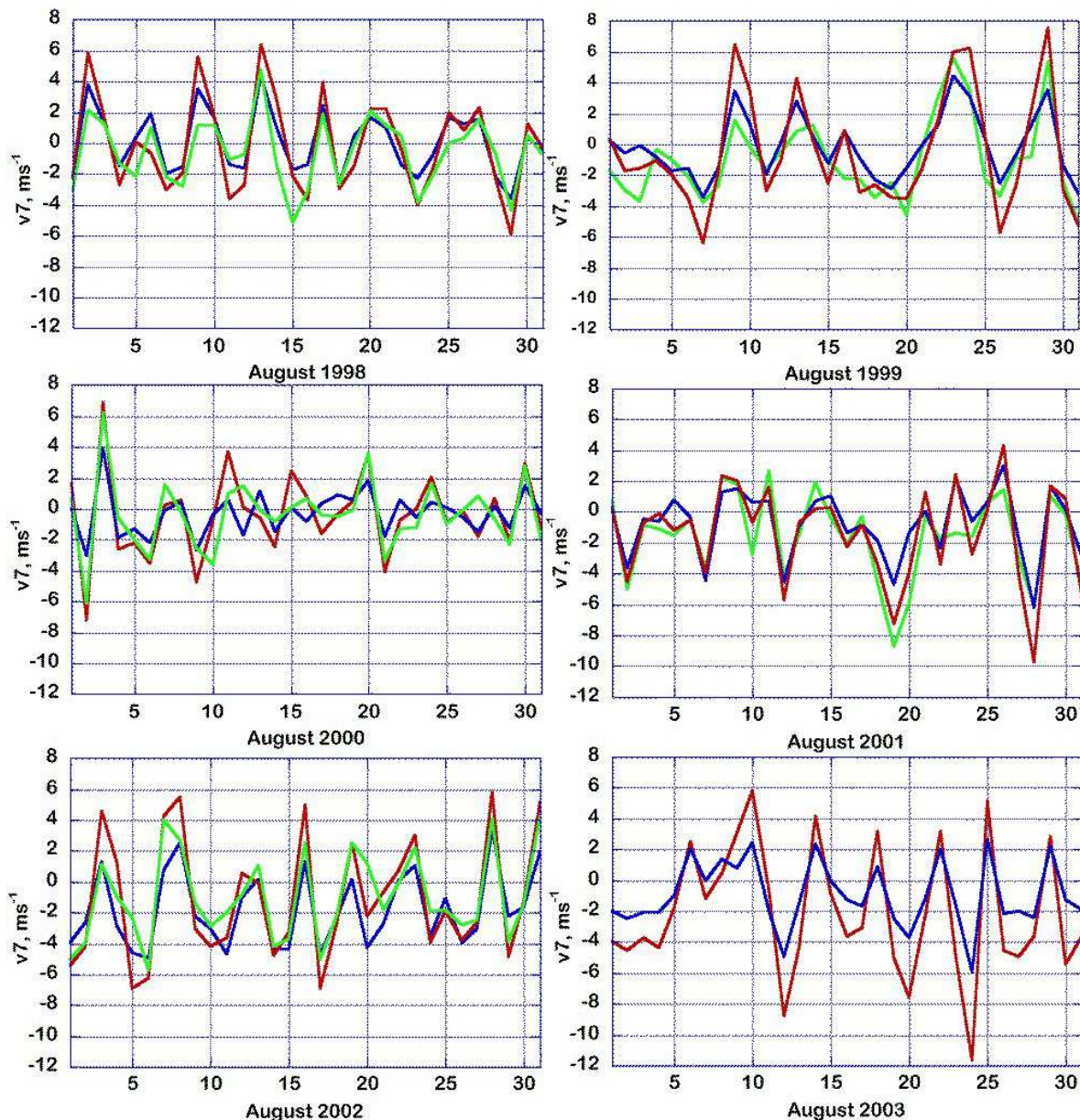


Fig. 4. Time series of v_7 along 7°W, averaged over 5-15°N, for each of six Augusts. Simulated RM3 16L v_7 (blue) are compared to NCPR v_7 (red) from the same data set as the lateral boundary conditions and to ERA-40 v_7 (green) (except for 2003).

Periodicities in v_7 associated with AEWs are evident. RM3 v_7 daily variability is highly correlated with corresponding NCPR (correlations ranging from 0.86 to 0.97) and ERA-40 values (correlations ranging from 0.76 to 0.86), but the RM3 v_7 amplitudes in Fig. 4 are the lowest of the three. Although the RM3 simulations are driven by NCPR data at the lateral

boundaries (LBC), circulation within the domain is entirely the product of the RM3 integration. The implication is that, based on the LBC, the RM3 generates and propagates the actual AEWs through the domain. Druryan et al. (2008) show that the spectral amplitudes and vorticity variances associated with RM3 AEWs double in amplitude between the eastern boundary and the center of the domain, so the model is not merely transporting an existing signal from NCPR westward.

3.4 Simulation of the seasonal march of precipitation

Precipitation over the Gulf of Guinea coast (about 6°N) typically wanes near the end of June and thereafter reforms over the Sahel closer to 10°N. Rapid advance of precipitation northward to the Sahel region during late June or early July, termed “onset”, is discussed by Hagos and Cook (2007), Sultan and Janicot (2000) and Ramel et al. (2006). Onset is related to

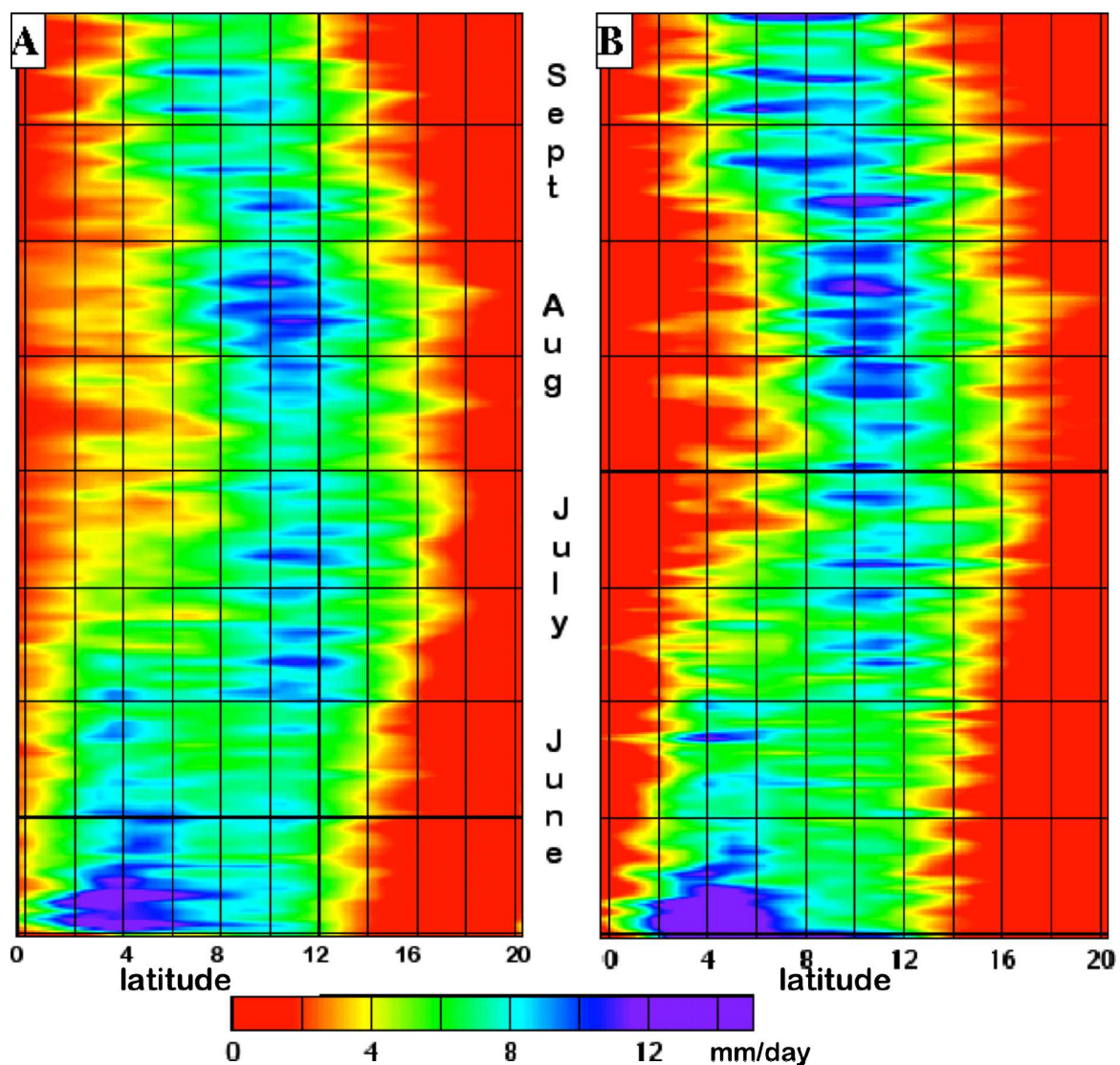
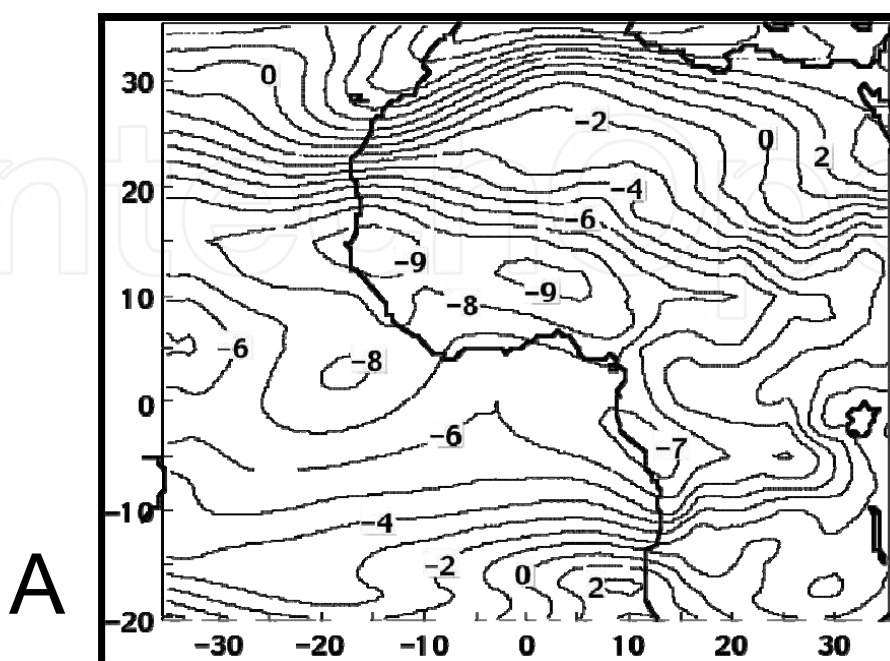


Fig. 5. Hovmöller time-latitude distributions of daily precipitation rates (mm day^{-1}) averaged over 15°W-10°E for June-September 1998-2003. a. RM3, b. TRMM (courtesy of NASA's Goddard Earth Sciences [GES] Data and Information Services Center).

increased continental sensible heating which, in turn, initiates a surge in moisture convergence over the Sahel. The ability of RCMs to reproduce the northward migration of the rain belt and its subsequent retreat is fundamentally important to both their usefulness in forecasting and climate sensitivity studies. Skillful simulation of the northward jump is especially desirable since it represents the onset of monsoon rains over the semi-arid Sahel region. Fig. 5a shows the latitude versus time progression of RM3 16L precipitation averaged over 15°W-10°E and over six seasons and Fig. 5b shows the corresponding graphic for TRMM data. The abrupt shift of heavy rainfall from 4°N to 10°N at the end of June is prominent on both panels. Moreover, the RM3 16L simulates the onset and other meridional shifts in the West African rain band in close agreement with TRMM observations.

3.5 The impact of increasing RM3 vertical resolution

Six June-September seasons simulated by the RM3 16L are compared to the corresponding simulations using the RM3 28L in Druyan et al. (2008). In general, the increased vertical resolution creates stronger circulation, manifest by a stronger African Easterly Jet (AEJ), stronger near-surface monsoon westerlies, stronger v7 spectra and stronger vorticity centers. Fig. 6 compares the 5-season mean zonal wind (m s^{-1}) at 700 mb for the two model versions, where the AEJ is represented by the diagonal swath of minimum zonal wind over West Africa. Corresponding NCPR zonal wind speeds (on the 2.5° grid) are intermediary between the 16L and 28L values, but the higher resolution RM3 28L may be a better representation of the actual circulation. Figs. 7a and 7b show the spatial distributions of vorticity of the 700 mb circulation by the 16L and 28L resolutions, respectively, for a composite of seven events that feature an AEW trough near 10°W. Each of these events occurs in both the 28L and 16L simulations. The positive and negative vorticity centers are about 50% more extreme for the 28L version, mostly because of stronger overall circulation. Higher vertical resolution does not have an impact on simulating the timing of monsoon onset.



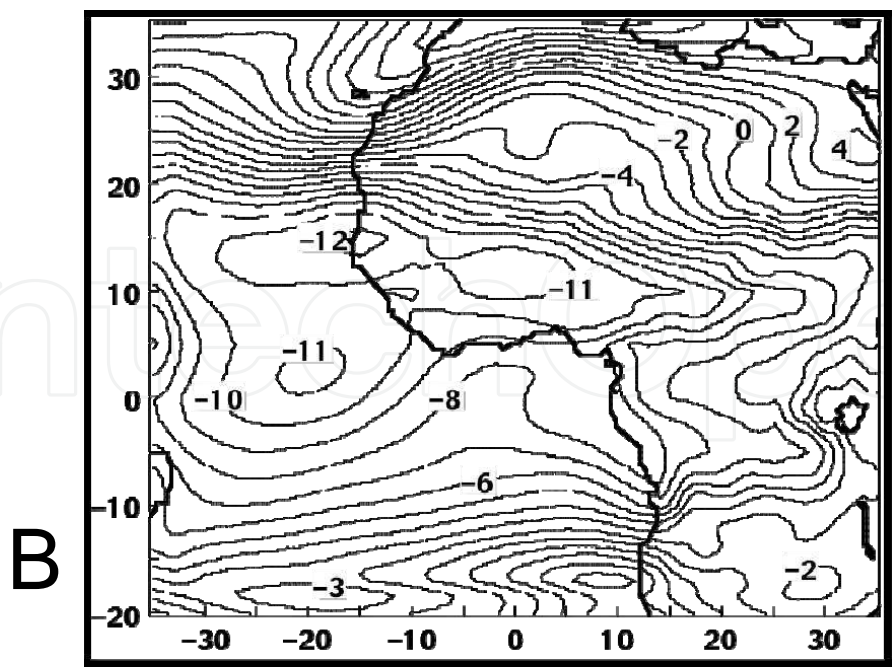


Fig. 6. Horizontal distributions of RM3 zonal winds (m s^{-1}) averaged over June-September 1998-2003. a. 16L, b. 28L.

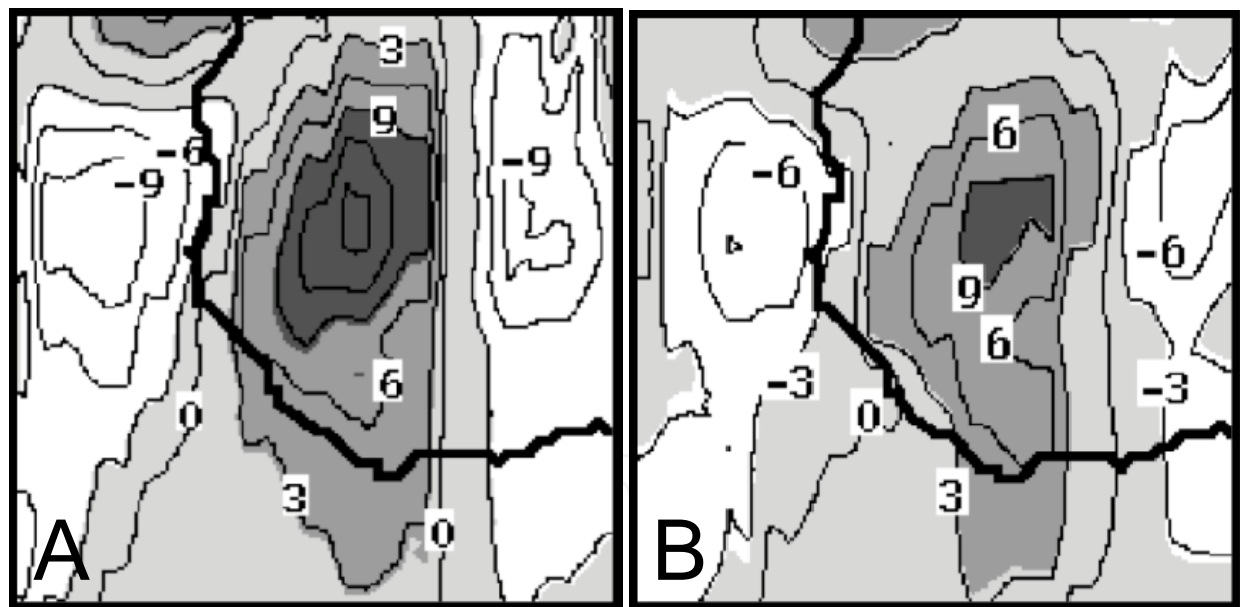


Fig. 7. Vorticity of the RM3 simulated 700 mb circulation for composites of seven events featuring an AEW near 10°W . a. RM3 16L, b. RM3 28L. Units: $\times 10^{-6} \text{ s}^{-1}$.

Druyan and Fulakeza (2011) used the RM3 28L to investigate the influence of the eastern tropical Atlantic SST maximum on the WAM climate, and in particular on transient AEWs. A control simulation was forced with May-October 2006 SST from NCPR2 and a second simulation experiment with the same forcing, except for -3°K SST anomalies between $0-15^{\circ}\text{N}$. Subtracting 3°K from the SST boundary conditions at every time step eliminated the SST maximum in the eastern tropical Atlantic. Both simulations were driven by the same

synchronous NCPR2 atmospheric lateral boundary data and both reproduced realistic ITCZ precipitation maximums and the actual transient AEWs with their associated rain shields. Fig. 8 shows time series of daily precipitation from each of the two experiments over the eastern tropical Atlantic (5-15°N, 25°W). The precipitation peaks in Fig. 8 represent the passage of convective complexes, presumably associated with AEWs. Results show that the absence of the SST maximum does not affect the timing of the precipitation systems, but rather the amplitude of each rain event. Fig. 8 shows that in the absence of the SST maximum, each precipitation peak is diminished, for example, on September 9th by some 83% and on September 12th by only about 10%.

4. WAMME

RM3 28L simulations are included in the West African Monsoon Modeling and Evaluation (WAMME) project, a recognized sub-group within the African Monsoon Multidisciplinary Analysis (AMMA) (Redelsperger et al., 2006). Druyan et al. (2010) summarized WAMME results from five regional models simulating the West African summer monsoon with both reanalysis and GCM forcing.

WAMME makes an intercomparison of the results from five RCMs including the RM3, each driven by synchronous NCEP reanalysis II and C20C SST data over four May- October seasons. The second part of the study analyzes results from two of the RCMs, driven with GCM (HadAM3) forcing, but the same SST lower boundary conditions.

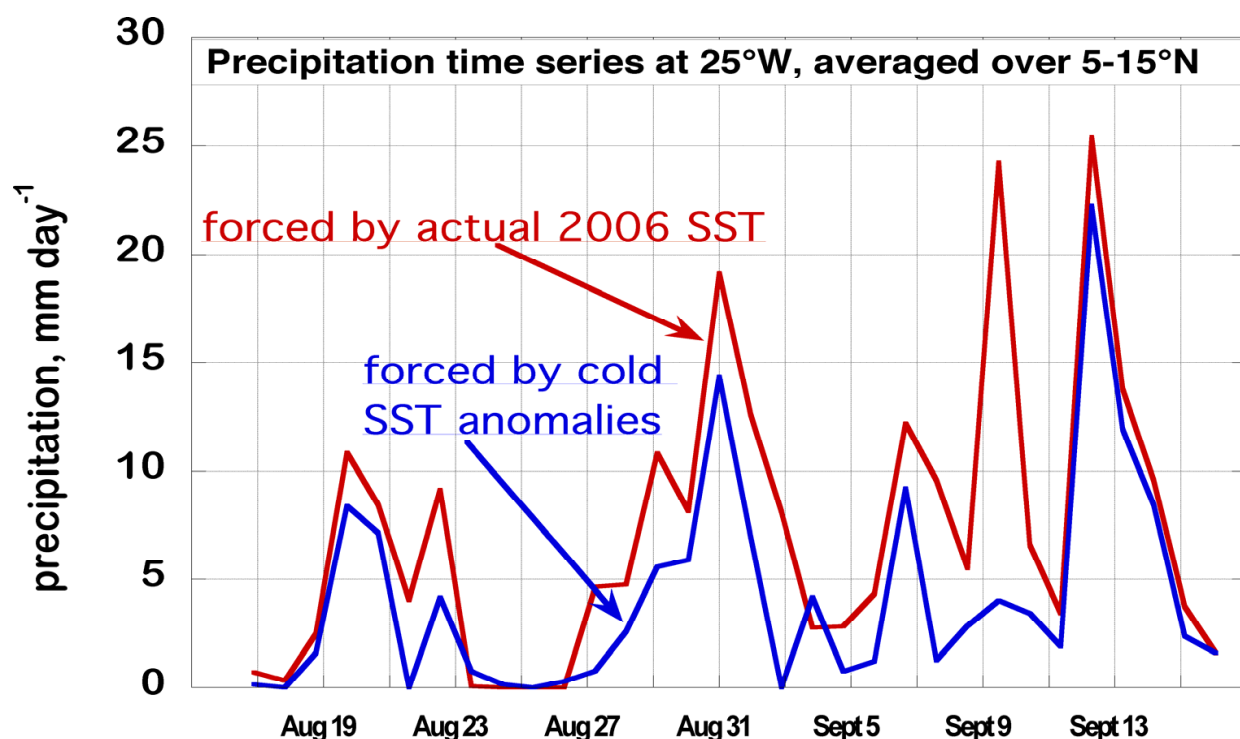


Fig. 8. Daily precipitation time series for two RM3 28L simulations at 25°W, averaged over 5-15°N. The red curve represents the August 16-September 16 interval from a May-September 2006 simulation forced with NCPR2 SST. The blue curve represents the same interval from a May-September 2006 simulation forced with NCPR2 SST minus 3°K between 0°-15°N.

The RCMs in the WAMME study simulate the northward jump of the precipitation band that represents monsoon onset over Sahelian Africa. However, the jumps in three of the four models are 2-5 weeks earlier than observed, suggesting serious model limitations for predicting monsoon onset. The RCMs show positive precipitation biases over much of West Africa, consistent with positive precipitation biases within the West African rain belt in NCEP reanalysis II and HadAM3 (Xue et al., 2010), the two data sets used for LBC. A five-model average precipitation bias for June-September mean rates over West Africa (5-20°N, 15°W-20°E) was about 1.7 mm day⁻¹ and the average spatial correlation between modeled and observed mean rainfall rates over the same area was 0.82, which means that the simulated pattern accounts for 67% of the observed spatial variance. Much of that success comes from correctly locating orographic precipitation maxima, the latitude of the main west to east rain band and the transition to the desert regime to the north. RCM performance in simulating the seasonal mean precipitation distribution compared to observations was generally better north of 10°N. Spatial correlation coefficients against the observed pattern are near 0.90 for all RCMs within the Sahel belt centered on 15°N, but are in the range of 0.30 to 0.65 for more southerly sub-regions. The four-model average surface air temperature bias for June-September means over West Africa (5-20°N, 15°W-20°E) is -2.6°K and the average spatial correlation between modeled and observed mean surface air temperature is 0.88. RM3 convective rainfall rates are excessive even with reasonable meridional moisture advection, while they are closer to observations with diminished moisture advection, suggesting the need to better optimize the convective parameterization.

5. Research outlook

WRF: We are creating and analyzing simulations of the West African summer monsoon using the Weather, Research and Forecasting (WRF) regional model and comparing results to RM3 performance. WRF is the product of considerable research and development (coordinated at the National Center for Atmospheric Research) and is considered to be state-of-the-art in sophistication. WRF is widely used for many climate research applications. However, to date there have been few applications of WRF in WAM studies. Moreover, there is no consensus yet on which combination of the many available alternative physical parameterizations for WRF is best suited for WAM studies. Erik Noble is heading this research effort.

ACMAD: We have collaborated with the African Center of Meteorological Application for Development (ACMAD), in Niamey, Niger, since 2005. ACMAD is a consortium of more than 50 African countries charged with providing meteorological and climate data to the constituent societies. The RM3 and supporting programs are installed at the ACMAD computing facility, producing daily weather forecasts that are posted on the ACMAD web site. The model is updated as needed via remote access. All RM3 simulations require initial conditions and boundary conditions, and those needed for the daily forecasts are downloaded from the Internet site of the US National Oceanic and Atmospheric Administration (NOAA). The system uses NOAA Global Forecast System data sets for initial conditions and boundary conditions, although special initialization techniques are required. Collaboration between CCSR/GISS and ACMAD compares RM3 forecasts of daily precipitation and surface temperature to co-located station observations. Results of this validation are not yet available.

Dr. Patrick Lonergan installed a program to automatically initiate the download of boundary condition data at designated appropriate times within the 24-hr cycle. Weather simulations are rather time consuming, but need to be timely if they are to be useful. The automation, using “crontabs,” is particularly valuable in that it allows the simulation jobs to get set up and completed overnight as the data becomes available, so that the forecasts can be finished early during the day shift. Posting of RM3 forecasts on the ACMAD website is interrupted by frequent down time of the internet connection and even the electric power supply.

CORDEX: RM3 simulations are underway for planned participation in the Africa subproject of the Coordinated Regional Climate Downscaling Experiment (CORDEX). CORDEX is an initiative of the World Climate Research Project (WCRP) of the UN. It aims to improve coordination of international efforts in regional climate downscaling, both by dynamical and statistical methods. Results for Africa are intended to provide support for the Intergovernmental Panel on Climate Change (IPCC) 5th Assessment Report (AR5), due out by 2013-2014. In the first phase, lateral boundary conditions (LBC) for driving the RM3 are taken from a $0.75^\circ \times 0.75^\circ$ gridded version of the European Center for Medium Range Weather Forecasts (ECMWF) interim reanalysis (ERA-I), available for the base period 1989-2008. Subsequently, LBC will be derived from atmosphere-ocean global model (AOGCM) climate change projections (from the Coupled Model Intercomparison Project [CMIP5]), for the future climate and for the base period. RM3 simulations covering all of Africa for the complete annual cycle will be provided to the CORDEX archive, which will facilitate model intercomparisons and multi-model ensemble/consensus results. Preliminary results (Jones and Nikulin 2011; Jones et al., 2011) show that 4 of the 5 RCMs (not including RM3) simulate too rapid an onset of summer monsoon rains near 10°N , based on validation of 1998-2008 simulations.

Fig. 9a shows some preliminary results of the RM3 simulation over the CORDEX domain (which encompasses all of Africa) driven by ERA-I and initialized on November 30, 1990. No adverse lateral boundary effects are evident in this precipitation rate difference field, nor in the monthly mean fields on which Fig. 9a is based (not shown). August 1991 minus January 1991 differences in precipitation rate reflect the migration of the rain belt from southern Africa in January, northward to northern hemisphere Africa in August. Fig. 9a, accordingly, features large gains over the Sahel latitudes centered at 10°N , and large deficits over southern Africa. In addition, negative differences along 5°S - 3°N over the Atlantic and Gulf of Guinea mark the vacated position of the January rain band during northern hemisphere summer. Fig. 9b shows the corresponding difference distribution based on CMAP (Climate Prediction Center Merged Analysis of Precipitation) data (Xie and Arkin, 1997). The CMAP observations validate the latitudes and orientation of the major RM3 difference extremes, evidence that the RM3 performs the seasonal transitions well. Excess positive RM3 differences in the Sahel reflect RM3 overestimates of August rainfall, although some of the higher RM3 values may be a consequence of the higher horizontal resolution that resolves orographic maxima better than CMAP, which is represented on a 2.5° grid. RM3 projections of climate change to be made in future research will be evaluated in the context of the performance for recent climate history.

Decadal climate change will generally warm near-surface air temperatures. Impacts on regional hydrology are less certain. Druyan (2011) reviews 10 climate model

investigations of 21st century trends of Sahel rainfall. There is no consensus among the studies as to whether climate change during this century will favor more frequent Sahel droughts or rainier summers. In order to properly simulate decadal precipitation trends for the Sahel a number of competing physical influences must be accurately considered by climate models. Perhaps the most challenging influence is to account for the future pattern of SST in the Atlantic Ocean. During the 20th century, cold (warm) SST anomalies in the tropical North Atlantic in juxtaposition with warm (cold) anomalies south of the Equator favored Sahel drought (positive rainfall anomalies) (Hastenrath and Polzin, 2010). If this teleconnection continues over the following decades, models will have to accurately project the sign and magnitude of the cross-equatorial SST gradient in the eastern Atlantic, which is a daunting challenge. Atmospheric and SST predictions from atmospheric-ocean global climate models (AOGCMs) forced by greenhouse gas trend scenarios will be used as the boundary conditions for regional model simulations. Results will therefore be derived from the latest generation of CMIP5 AOGCMs’ projections of SST and atmospheric conditions, downscaled by regional models to provide climate evolution scenarios with high spatial detail over West Africa. The regional models, in turn, will then simulate high resolution projections of the West African climate that account for other forcings, among them projected changes in land use and vegetation cover. This line of research will accordingly test the sensitivity of climate change over West Africa to desertification, deforestation, changes in cropland, urbanization, etc.

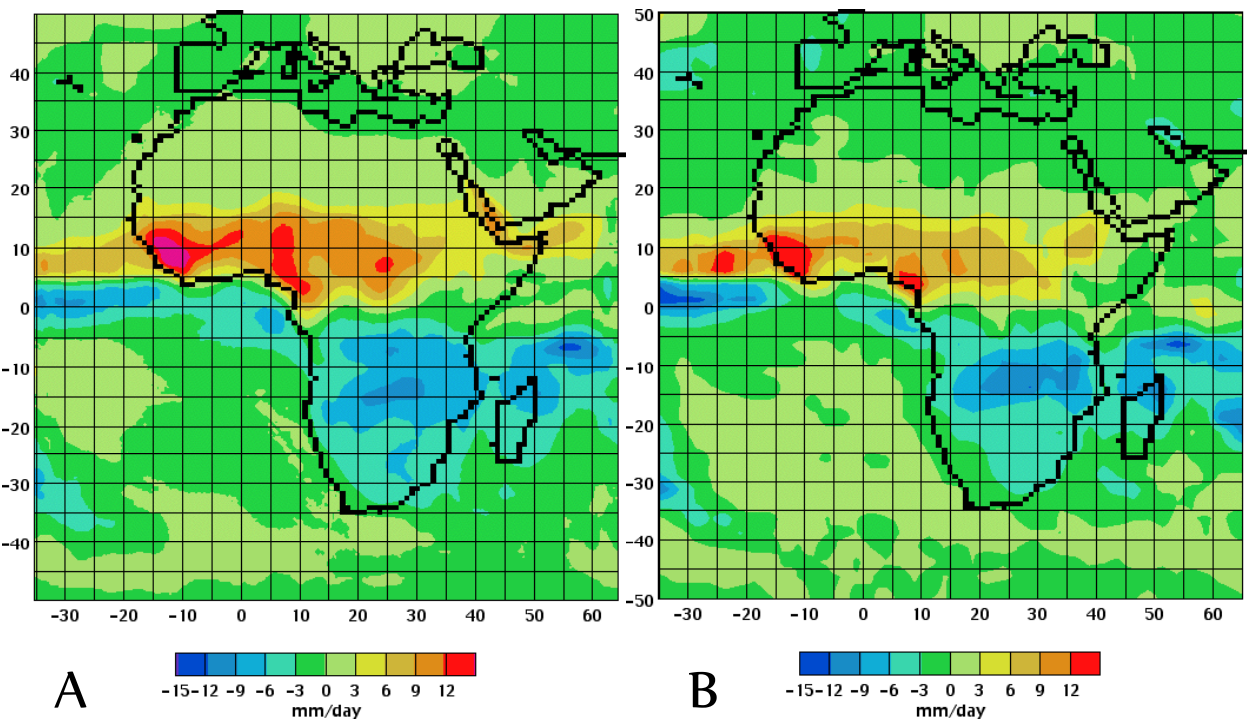


Fig. 9. August 1991 minus January 1991 precipitation rate differences (mm day⁻¹).
a. RM3 driven by ERA-I data; b. CMAP observations (gridded at 2.5°, data courtesy of the Earth System Research Laboratory, Physical Sciences Division, NOAA).

6. Acknowledgments

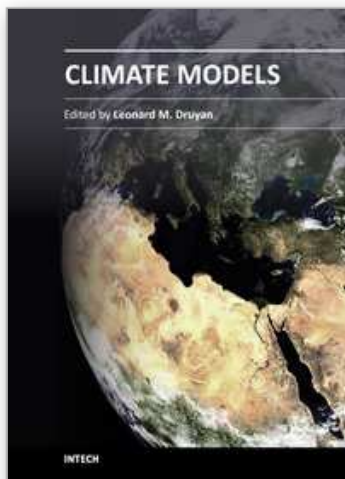
Research reported here was supported by National Science Foundation grants AGS-0652518 and AGS-1000874, NASA grant NNX07A193G and NASA cooperative agreement NNG04GN76A. TRMM images and data are acquired using the GES-DISC Interactive Online Visualization AND aNalysis Infrastructure (Giovanni) as part of the NASA's Goddard Earth Sciences (GES) Data and Information Services Center (DISC). Reanalysis and CMAP data are provided by the NOAA-ESRL Physical Sciences Division, Boulder Colorado from their Web site at <http://www.esrl.noaa.gov/psd/>.

7. References

- Druyan L (2011) Studies of 21st century precipitation trends over West Africa. *Int. J. Climatology* 31: 1415-1424. DOI: 10.1002/joc.2180.
- Druyan, L., M. Fulakeza, and P. Lonergan (2006) Mesoscale analyses of West African summer climate: Focus on wave disturbances. *Clim Dyn* 27: 459-481. doi:10.1007/s00382-006-0141-9.
- Druyan, L., M. Fulakeza, and P. Lonergan (2008) The impact of vertical resolution on regional model simulation of the West African summer monsoon. *Int. J. Climatology*, 28: 1293-1314 doi:10.1002/joc.1636.
- Druyan L, Fulakeza M (2011) The sensitivity of African easterly waves to eastern tropical Atlantic sea-surface temperatures. *Meteorol. Atmos. Phys.* 113: 39-53. DOI 10.1007/s00703-011-0145-9
- Druyan L.M.; J. Feng; K.H. Cook; Y. Xue; M. Fulakeza; S.M. Hagos; A. Konare; W. Moufouma-Okia; D.P. Rowell; E.K. Vizy (2010) The WAMME regional model intercomparison study. *Clim Dyn* 35, 175-192. DOI 10.1007/s00382-009-0676-7.
- Hansen J, co-authors (2002) Climate forcings in Goddard Institute for Space Studies SI2000 simulations. *JGR* DOI: 10.1029/2001JD001143
- Hagos S M, Cook KH (2007) Dynamics of the West African Monsoon Jump. *J Clim* 20: 5264-5284.
- Hastenrath S, Polzin D (2010) Long-term variations of circulation in the tropical Atlantic sector and Sahel rainfall. *Int. J. Climatol.* DOI: 10.1002/joc.2116.
- Jones C, Nikulin G (2011) Evaluating the first CORDEX simulations over Africa. http://www.smhi.se/forskning/forskningsomraden/klimat_forskning/1.11299.
- Jones C, Giorgi F, Asrar G (2011) The Coordinated Regional Downscaling Experiment: CORDEX, an international downscaling link to CMIP5. *CLIVAR Exchanges* 16: 34-39.
- Kanamitsu M, Ebisuzaki W, Woollen J, Yang S K, Hnilo J J, Fiorino M, Potter G L (2002) NCEP-DOE AMIP-II reanalysis (R-2). *Bull Am Meteor Soc* 83: 1631-1643.
- Kummerow C, co-authors (2000) The status of the Tropical Rainfall Measuring Mission (TRMM) after two years in orbit. *J. Appl. Meteor.* 39: 1965-1982.
- New M, Lister D, Hulme M, Makin I, 2002: A high-resolution data set of surface climate over global land areas. *Clim Res* 21: 1-25.
- Ramel R, Gallée H, Messenger C (2006) On the northward shift of the West African monsoon. *Clim Dyn* 26: 429-440. DOI 10.1007/s00382-005-0093-5
- Redelsperger JL, C.D. Thorncroft, A. Diedhiou, T. Lebel, D.J. Parker, J. Polcher (2006) African monsoon multidisciplinary analysis: an international research project and field campaign. *Bulletin of AMS* 87: 1739-1746.

- Rosenzweig C, Abramopoulos F (1997) Land-surface model development for the GISS GCM. *J Climate* 10: 2040-2054.
- Sultan B, Janicot S (2000) Abrupt shift of the ICTZ over West Africa and intra-seasonal variability. *Geophys Res Lett* 27: 3353–3356.
- Thorncroft and co-authors (2003) The JET2000 Project: Aircraft observations of the African Easterly Jet and African easterly waves. *Bull Am Met Soc* 84: 337-351.
- Xie, P., and P.A. Arkin, 1997: Global precipitation: A 17-year monthly analysis based on gauge observations, satellite estimates, and numerical model outputs. *Bull. Amer. Meteor. Soc.*, 78, 2539 - 2558.
- Xue Y et al. (2010) Intercomparison of West African monsoon and its variability in WAMME: First GCM experiment. *Clim Dyn* 35: 3-27.

IntechOpen



Climate Models

Edited by Dr. Leonard Druyan

ISBN 978-953-51-0135-2

Hard cover, 336 pages

Publisher InTech

Published online 02, March, 2012

Published in print edition March, 2012

Climate Models offers a sampling of cutting edge research contributed by an international roster of scientists. The studies strive to improve our understanding of the physical environment for life on this planet. Each of the 14 essays presents a description of recent advances in methodologies for computer-based simulation of environmental variability. Subjects range from planetary-scale phenomena to regional ecology, from impacts of air pollution to the factors influencing floods and heat waves. The discerning reader will be rewarded with new insights concerning modern techniques for the investigation of the natural world.

How to reference

In order to correctly reference this scholarly work, feel free to copy and paste the following:

Leonard M. Druyan and Matthew Fulakeza (2012). Regional Climate Model Applications for West Africa and the Tropical Eastern Atlantic, Climate Models, Dr. Leonard Druyan (Ed.), ISBN: 978-953-51-0135-2, InTech, Available from: <http://www.intechopen.com/books/climate-models/regional-climate-model-applications-for-west-africa>

INTech
open science | open minds

InTech Europe

University Campus STeP Ri
Slavka Krautzeka 83/A
51000 Rijeka, Croatia
Phone: +385 (51) 770 447
Fax: +385 (51) 686 166
www.intechopen.com

InTech China

Unit 405, Office Block, Hotel Equatorial Shanghai
No.65, Yan An Road (West), Shanghai, 200040, China
中国上海市延安西路65号上海国际贵都大饭店办公楼405单元
Phone: +86-21-62489820
Fax: +86-21-62489821

© 2012 The Author(s). Licensee IntechOpen. This is an open access article distributed under the terms of the [Creative Commons Attribution 3.0 License](https://creativecommons.org/licenses/by/3.0/), which permits unrestricted use, distribution, and reproduction in any medium, provided the original work is properly cited.

IntechOpen

IntechOpen